Computers, Materials & Continua
DOI: 10.32604/cmc.2023.035964
Article

Tech Science Press

An Efficient EMD-Based Reversible Data Hiding Technique Using Dual Stego Images

Ahmad A. Mohammad*

Princess Sumaya University for Technology, Amman, 11941, Jordan
*Corresponding Author: Ahmad A. Mohammad. Email: atawayha@psut.edu.jo

Received: 12 September 2022; Accepted: 08 December 2022

Abstract: Exploiting modification direction (EMD) based data hiding techniques (DHTs) provide moderate data hiding capacity and high-quality stego images. The overflow problem and the cyclic nature of the extraction function essentially hinder their application in several fields in which reversibility is necessary. Thus far, the few EMD reversible DHTs are complex and numerically demanding. This paper presents a novel EMD-based reversible DHT using dual-image. Two novel 2×4 modification lookup tables are introduced, replacing the 256×256 reference matrix used in similar techniques and eliminating the numerically demanding search step in similar techniques. In the embedding step, one of the modification tables modifies a pixel in odd columns in the first cover image and keeps its image in the second cover image intact. The other modification table modifies a pixel in even columns in the second cover image and keeps its image in the first cover image intact. This embedding strategy enables direct reversibility at almost zero computational cost. This technique embeds one $4 - ary$ secret digit into each pixel in the first cover image and its image in the second cover image resulting in one bit per pixel (bpp) data embedding rate. The use of the $4 - ary$ numbering system enables direct and numerically efficient conversion of the binary secret message to the $4 - ary$ and vice versa. The advantages of the proposed algorithm are straightforward reversibility, simplicity, numerical efficiency, direct conversion of the binary secret message to $4 - ary$ and vice versa, and elimination of the need for the 256×256 reference matrix by replacing it with two 2×4 lookup tables. Simulation results show that the embedding rate of the proposed technique is one bpp. It achieved more than 49 dB average Peak to Signal Noise Ratio (PSNR) over all test images.

Keywords: Reversible data-hiding; EMD-based; high capacity; steganography

1 Introduction

In the era of the internet, the internet of things (IoT), and mobile communications, the interchange of vast amounts of digital data has become an easy task. Some of this information includes some secret data. Unintended recipients can easily access this data. Thus, there is a need for the development of means to protect the transmitted data. Thus far, researchers have developed two main methods to achieve data protection: Data encryption [1] and Data hiding [2–43]. Data encryption techniques share the data in a meaningless form and can be easily identified as confidential data, making it vulnerable to attacks [2]. DHTs conceal the secret data in meaningful digital media (usually a digital image called a cover image). Depending on the nature of the hidden message, one can classify DHTs into two main categories: Digital watermarking, when the message is concerned with the cover, and steganography, otherwise [2]. Steganographic techniques transparently conceal the secret message into a cover object such as a digital image. The main objective of these techniques is to hide the mere existence of the secret message in the cover object. However, the concealment of the secret message in the cover object produces a distorted stego object with reduced visual quality. Steganographic techniques should keep the distortion minimal and transparent so it cannot be detected. Another important objective in steganography is to increase the data hiding capacity, defined as the number of secret message bits embedded in the cover object. However, increasing data hiding capacity introduces more distortions in the cover image, reducing visual quality and destroying transparency. Thus, there is a need for a tradeoff between transparency and data-hiding capacity [3]. DHTs may also be classified as irreversible [3–23] and reversible [24–43]. In irreversible DHTs, the distortions to the cover object are permanent, and one can't restore the original cover object after extracting the secret message. In reversible DHTs, the distortions to the cover image are not permanent, and one can restore the original cover image after extracting the secret message. The reversibility of DHTs is necessary for some applications, such as military, law enforcement, and medical applications. DHTs are numerous and may be carried out in the spatial or transform domains [3]. In the spatial domain, one can find several methods, such as Image interpolation, Difference expansion (D.E.), Histogram shifting (H.S.), Least significant bit substitution (LSB), and EMD-based methods [3].

The EMD-based methods have some attractive features: They provide high-quality stego images and can attain relatively high embedding rates. EMD-based techniques have witnessed extensive research efforts [4–36]. Reference [8] introduced the first EMD-based technique, partitioning the cover image into groups of n-pixels; they embedded a $(2n + 1) - ary$ secret digit into each group of n-pixels by increasing or decreasing the value of only one pixel in the group by one. The stego image quality is relatively low. Reference [9] proposed an Improved EMD (IEMD) method in which they were able to increase the embedding rate up to 1.5 bits per pixel (bpp) while maintaining good-quality stego images. Reference [10] introduced the diamond encoding technique in which they embed a $\left(2k^2 + 2k + 1\right) - ary$ secret digit into a pair of cover pixels. The embedding parameter k controls the embedding rate. The image quality becomes low as k goes high. Reference [12] proposed a fully EMD technique (FEMD), in which they utilized a new extraction function and increased the data hiding capacity up to 4.5 bpp. However, the image quality is low. Reference [13] proposed a formula FEMD (FFEMD) in which they eliminated the need for the 256 × 256 matrix function table needed in the FEMD method. However, numerical complexity is increased. Reference [14] combined difference expansion and FFEMD to improve the data hiding capacity and image quality. They have also proposed a solution to the overflow problem in EMD-based techniques. Reference [15] proposed a method to embed an $n^2 - ary$ secret digit into each group of n pixels obtaining up to a four bpp embedding rate. This method is similar to the IEMD scheme, with a slight improvement in image quality. The above-mentioned EMD-based algorithms are irreversible and numerically demanding. Due to the extraction function's cyclic nature, most EMD-based DHTs are irreversible, and one can find a few reversible EMD-based DHTs [24–43]. Reference [24] proposed the first reversible EMD-based DHT using two stego images. They insert A $5 - ary$ secret digit into two consecutive pixels of the two cover images. The algorithm is somewhat numerically demanding, provides an embedding rate of one bpp, and high-quality stego images of

45 dB PSNR values. Reference [25] proposed an EMD-based reversible DHT using two stego images. They insert A $5-ary$ secret digit into one pixel in the first cover image and its dual image in the second cover image. The algorithm is numerically demanding and provides an embedding rate of 1.55 bpp and stego images of 38 dB PSNR values. Reference [27] proposed an adaptive EMD-based reversible DHT using two stego images. Using a $9 - ary$ numeral system, they inserted two secret digits into two adjacent pixels in the first and second cover images. The algorithm is numerically demanding, provides an embedding rate of 1.55 bpp, and stego images quality of 43 dB PSNR values. Reference [28] proposed an EMD-based reversible DHT using two stego images. They insert a $9-ary$ secret digit into one pixel in the first cover image and its dual image in the second cover image. The algorithm is numerically demanding and provides an embedding rate of 1.55 bpp and stego images of 38 dB PSNR values. Reference [29] proposed an EMD-based reversible DHT using two stego images. Using a $9-ary$ numeral system, they inserted two secret digits into two adjacent pixels in the first and second cover images. The algorithm is numerically demanding and provides an embedding rate of 1.55 bpp and stego image quality of 43 dB PSNR values. Reference [30] proposed a reversible DHT using an orientation combination of dual stego images. Using a $25 - ary$ numeral system, they inserted a secret digit into two adjacent pixels in each stego image. The algorithm is numerically demanding and provides an embedding rate of 1.14 bpp and stego image quality of 50 dB PSNR values. Reference [31] proposed an adaptive EMD-based reversible DHT using two stego images. Using a $5-ary$ numeral system, they inserted two secret digits into two adjacent pixels in the first and second cover images. The algorithm is numerically demanding and provides an embedding rate of 1 bpp and stego image quality of 50 dB PSNR values. Reference [32] proposed an RDHT using an orientation combination of dual stego images. Using a $52-ary$ numeral system, they inserted two secret digits into two adjacent pixels in the two stego images. The algorithm is numerically demanding and provides an embedding rate of 1.58 bpp and stego images quality of 45 dB PSNR values. Reference [38] proposed a numerically efficient RDHT using two shadow images. Using a combination of $2-ary$ and $5-ary$ numeral systems, they obtained an embedding rate of 1.56 bpp and stego images quality of 43 dB PSNR values. However, the algorithm needs the 256 × 256 reference matrix. Reference [40] proposed an RDHT using three shadow images. Using a combination of $5-ary$ and $6-ary$ numeral systems, they obtained an embedding rate of 1.13 bpp and stego images quality of 48 dB PSNR values. However, the algorithm is somewhat complex and requires the transmission of side information to achieve reversibility. Reference [42] proposed an adaptive turtle-shell-based RDHT using dual images. Using an $8-ary$ numeral system, they obtained an embedding rate of 1.25 bpp and stego images quality of 45 and 49 dB PSNR values. Again, the algorithm is numerically demanding. All these methods use two or more cover images and improve security via secret key sharing [44].

We summarize our findings by the following points:

- Due to the cyclic nature of the extraction function and the overflow problem, EMD-based DHTs are not directly reversible
- EMD-based DHTs can provide high embedding rates. However, increasing the embedding rate decreases the stego image quality
- In general, increasing embedding rates above two bpp results in significant distortions in the stego image, making it vulnerable to detection
- Researchers proposed the use of dual images to develop reversible EMD-based DHTs
- The use of dual images increases the security of the secret data via secret key sharing
- Thus far, existing dual image-based EMD-based reversible DHTs are numerically demanding, require complex search algorithms, and need to generate a 256 × 256 reference matrix

This paper presents an EMD-based reversible DHT using dual stego images. The contributions of our technique are:

- Simple and numerically efficient embedding and extraction algorithms
- Relatively high data-hiding capacity
- Direct and numerically efficient conversion of the binary secret message to $4 - ary$ and vice versa
- Elimination of the need for the 256 × 256 reference matrix used in similar techniques by replacing it with novel two 2 × 4 lookup tables, and elimination of the need for the complex and numerically demanding search step required by similar techniques
- An embedding strategy that enables straightforward reversibility with almost zero computational cost
- Increased Security by using secret key sharing and the equal high-quality of the two stego images

The rest of this paper proceeds as follows. In Section 2, we give a summary of some related work. Section 3 outlines the proposed algorithm, the data-hiding step, and the data extraction and image recovery step. Section 4 gives experimental simulation results. Finally, Section 5 presents the discussion, conclusion, and future work.

2 Background

This section presents the fundamentals of EMD-based DHTs and gives details of some related techniques.

2.1 Fundamentals of EMD-Based DHTs

These schemes conceal an $l - ary$ secret digit in a group of n-pixels of the $M \times N$ cover image I. The first step in these schemes is to segment I into groups of n-pixels. The extraction function takes the form $f_e\left(x_1, x_2, \ldots, x_n\right) = \left(\sum_{i=1}^{n} a_i \times x_i\right) mod\ l$ where a_is and l are positive integers. The extraction function $f_e\left(x_1, x_2, \ldots, x_n\right)$ is cyclic and has a range of 0 to $l - 1$ values. We refer to these values as characteristic values. Using the vector of pixels $v\left(x_1, x_2, \ldots, x_n\right)$ as the origin of an n-coordinate system, we search for a vector $v' = \left[x'_1, x'_2, \ldots, x'_n\right]$ within a neighborhood-set $\psi\left(x_1, x_2, \ldots, x_n\right)$. The new vector (stego vector) v' should satisfy the condition $f_e\left(x'_1, x'_2, .., x_s, ., x'_n\right) = s_l$; where s_l is the secret digit in the $l - ary$ number system. We define the neighborhood-set $\psi\left(x_1, x_2, \ldots, x_n\right)$ as the set of vectors $v_\psi = \left[p_1, p_2, \ldots, p_n\right]$ that satisfy a distance condition of the form $\sum_i \left|p_i - x_i\right| \leq k; k = 1, 2, 3, \ldots, l - 1$, or minimize a cost function $J = \left|vv^T - v'^T v'\right|$. We choose k such that each characteristic value occurs at least once over the set $\psi\left(x_1, x_2, \ldots, x_n\right)$. The distortion in $\psi\left(x_1, x_2, \ldots, x_n\right)$ should be minimal. Thus, we pick a small neighborhood set $\psi_l\left(x_1, x_2, \ldots, x_n\right)$ to satisfy: 1) There are precisely l elements in $\psi_l\left(x_1, x_2, \ldots, x_n\right)$, and 2) The values of $f_e\left(x_1, x_2, \ldots, x_n\right)$ over $\psi_l\left(x_1, x_2, \ldots, x_n\right)$ are mutually exclusive. Increasing n usually decreases the distortion and data hiding capacity. For this, the most commonly used value is $n = 2$. Fig. 1 shows some examples (patterns) of the neighborhood set ψ_l and the corresponding characteristic values. The second step is to embed an $l - ary$ secret digit into the vector $\left[x_1, x_2, \ldots, x_n\right]$ so that the distance between the original cover vector $\left[x_1, x_2, \ldots, x_n\right]$ and the resulting stego vector $\left[x'_1, x'_2, .., x_s, ., x'_n\right]$ is minimal. In the extraction step, the stego image pixels are segmented into a group of vectors $v' = \left[x'_1, x'_2, \ldots, x'_n\right]$ in the same order as that in the embedding step. The resulting secret message is: $s_l = f_e\left(x'_1, x'_2, .., x_s, ., x'_n\right)$ [11].

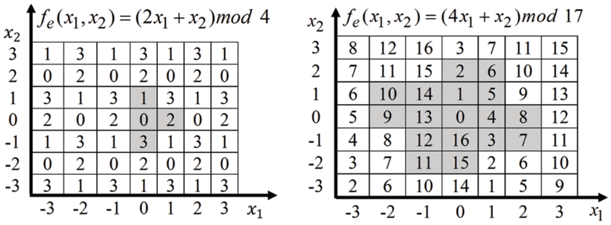
$f_e(x_1,x_2)=(2x_1+x_2)mod\ 4$
x_2
x_1
$f_e(x_1,x_2)=(4x_1+x_2)mod\ 17$
x_2
x_1

x_2							
3	1	3	1	3	1	3	1
2	0	2	0	2	0	2	0
1	3	1	3	1	3	1	3
0	2	0	2	0	2	0	2
-1	1	3	1	3	1	3	1
-2	0	2	0	2	0	2	0
-3	3	1	3	1	3	1	3
	-3	-2	-1	0	1	2	3 x_1

x_2							
3	8	12	16	3	7	11	15
2	7	11	15	2	6	10	14
1	6	10	14	1	5	9	13
0	5	9	13	0	4	8	12
-1	4	8	12	16	3	7	11
-2	3	7	11	15	2	6	10
-3	2	6	10	14	1	5	9
	-3	-2	-1	0	1	2	3 x_1

Figure 1: Neighborhood set for different extraction functions

2.2 *Related Work*

This section presents two closely related DHTs proposed by [8,31].

2.2.1 EMD Algorithm [8]

This scheme is the basis of EMD-based DHTs. It embeds a $(2n+1)-ary$ secret digit in a sequence of n-cover pixels. The algorithm starts by segmenting the cover image into blocks of n-non-overlapping pixels. In order to conceal the secret digit, only one of the n-pixels is increased or decreased by one. The extraction function used in the embedding and extraction phases is:

$f_e\,(x_1, x_2, \ldots, x_n) = \left(\sum_{i=1}^{n} i \times x_i\right) mod\ \ (2n+1)$; where x_i represents the ith pixel value, n is the number of pixels, and mod is the modulus operation. To embed a secret digit into a group of pixels $(x_1, x_2, \ldots, x_n)$, we find the difference $d = (s - f_e\,(x_1, x_2, \ldots, x_n))\ \mathrm{mod}(2n+1)$ and obtain the modified Block as follows:

```
If $d = 0$
    Set $\left(x'_1, x'_2, \ldots, x'_n\right) = (x_1, x_2, \ldots, x_n)$
ElseIf $d \leq n$
    Set $\left(x'_1, x'_2, .., x_s, ., x'_n\right) = (x_1, x_2, .., x_s + 1, .., x_n)$,
Else
    Set $\left(x'_1, x'_2, .., x_{2n+1-s}, ., x'_n\right) = (x_1, x_2, .., x_{2n+1-s} - 1, .., x_n)$
End.
```

At the receiver end, we extract the secret digit as $s = f_e\left(x'_1, x'_2, \ldots, x'_n\right) = \left(\sum_{i=1}^{n} i \times x_i\right) mod\ \ (2n+1)$. The hiding capacity for this scheme is $\left(\log_2(2n+1)\right)/n$ bpp. The maximum hiding capacity occurs when $n = 2$ with a 1.161 bpp embedding rate. This scheme is irreversible.

2.2.2 Reversibility Data Hiding [31]

Reference [31] proposed an EMD-based reversible DHT scheme using dual images. The extraction function is: $f_e\,(x_1, x_2) = (x_1 + 2x_2)\, mod\ \ 5$, where (x_1, x_2) are two adjacent pixels in the original cover image I. Fig. 2a shows the 256×256 reference matrix M. Fig. 2b shows a 3×3 block centered at pixel pair (x_1, x_2). They divide the block pixels into two distinct groups: G_1 and G_2. Each block contains nine positions labeled as: $l_1, l_2, \ldots, l_9$, as shown in Fig. 2b. G_1 consists of the positions $(l_2, l_4, l_5, l_6, l_8)$, while G_2 consists of the locations $(l_1, l_3, l_5, l_7, l_9)$. The algorithm embeds two $5 - ary$ secret digits (S_1, S_2) into each pair of pixels (x_1, x_2), resulting in two stego images $\left(x'_1, x'_2\right)$ and $\left(x''_1, x''_2\right)$. The algorithm starts by scanning the reference matrix M and obtaining the 3×3 block corresponding to the pixel pair (x_1, x_2). Then it locates the position of S_1 in G_1 and the position of S_2 in G_2. Denote the pixel values in these locations as $\left(x_{1p1}, x_{2p1}\right)$ and $\left(x_{1p2}, x_{2p2}\right)$. Let $S_d = (x_{2p1} - x_{1p1})^2 + (x_{2p2} - x_{1p2})^2$ be the square of the length of the line connecting these positions and find the stego pixels values using the following algorithm:

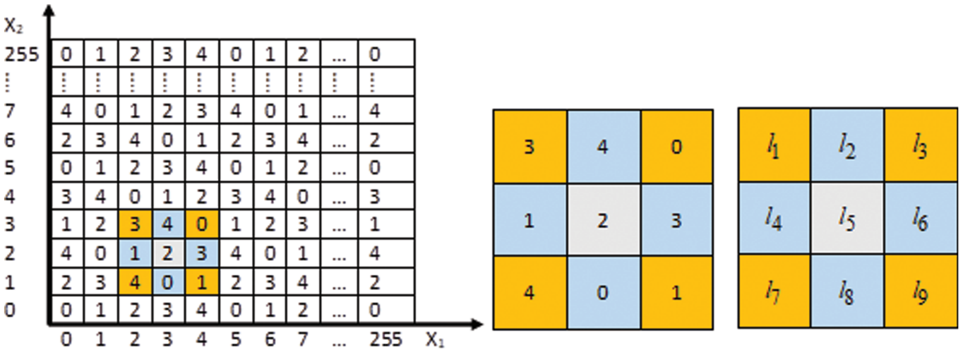

X_2										
255	0	1	2	3	4	0	1	2	...	0
⋮	⋮	⋮	⋮	⋮	⋮	⋮	⋮	⋮	⋮	⋮
7	4	0	1	2	3	4	0	1	...	4
6	2	3	4	0	1	2	3	4	...	2
5	0	1	2	3	4	0	1	2	...	0
4	3	4	0	1	2	3	4	0	...	3
3	1	2	3	4	0	1	2	3	...	1
2	4	0	1	2	3	4	0	1	...	4
1	2	3	4	0	1	2	3	4	...	2
0	0	1	2	3	4	0	1	2	...	0
	0	1	2	3	4	5	6	7	...	255 X_1

(a)

3	4	0
1	2	3
4	0	1

(b)

l_1	l_2	l_3
l_4	l_5	l_6
l_7	l_8	l_9

(c)

Figure 2: (a) Reference matrix (b) 3×3 block (c) 9 positions labeling

Embedding Algorithm [31]

```
If $(x_1 = 0)$ or $(x_1 = 255)$ or $(x_2 = 0)$ or $(x_2 = 255)$, then
        Do not embed the secret message. Set $\left(x'_1, x'_2\right) = (x_1, x_2)$ and $\left(x''_1, x''_1\right) = (x_1, x_2)$
ElseIf $(S_d = 0)$ or $(S_d = 2)$ or $(S_d = 5)$, then
        Set $\left(x'_1, x'_2\right) = \left(x_{1p1}, x_{2p1}\right)$ and $\left(x''_1, x''_2\right) = \left(x_{1p2}, x_{2p2}\right)$
ElseIf $S_d = 1$, then Set $\left(x''_1, x''_2\right) = \left(x_{1p2}, x_{2p2}\right)$.
    If $\left(x''_1, x''_2\right) = (x_1, x_2)$, then
            Set $\left(x'_1, x'_2\right) = \left(x_{1p1}, x_{2p1}\right)$
    ElseIf the line segment from $\left(x_{1p1}, x_{2p1}\right)$ to $\left(x_{1p2}, x_{2p2}\right)$ is clockwise, then
        Set $\left(x'_1, x'_2\right) = \left(2x_{1p1} - x_{1p2}, 2x_{2p1} - x_{2p2}\right)$
    Else
        Set $\left(x'_1, x'_2\right) = \left(2x_1 - x_{1p2}, 2x_2 - x_{2p2}\right)$
    End
End
```

Secret message extraction and original image recovery [31]

Given the two stego pixel pairs $\left(x'_1, x'_2\right)$ and $\left(x''_1, x''_2\right)$, resulting from the embedding step, find the distance $S_d = (x'_{2p1} - x'_{1p1})^2 + (x''_{2p2} - x''_{1p2})^2$. Next, recover the original pixel pair (x_1, x_2) and extract the secret digits (S_1, S_2) according to the following cases:

Case 1: $S_d = 0$;

```
    If $(x_1 = 0)$ or $x_1 = 255$, or $x_2 = 0$, or $x_2 = 255$), then
        Set $\left(x'_{1new}, x'_{2new}\right) = \left(x'_1, x'_2\right)$ and $(x_1, x_2) = \left(x'_1, x'_2\right)$. Do not extract any secret digits.
    Else
```

```
        Set $\left(x'_{1new}, x'_{2new}\right) = \left(x'_1, x'_2\right)$ and $(x_1, x_2) = \left(x'_1, x'_2\right)$. Extract the two secret digits from the reference matrix $M$ corresponding to $\left(x'_{1new}, x'_{2new}\right)$ and $\left(x'_1, x'_2\right)$.
    End
Case 2 $S_d = 1$;
    Set $\left(x'_{1new}, x'_{2new}\right) = \left(x'_1, x'_2\right)$ and $(x_1, x_2) = \left(x''_1, x''_2\right)$. Extract the two secret digits from the reference matrix $M$ corresponding to $\left(x'_{1new}, x'_{2new}\right)$ and $\left(x'_1, x'_2\right)$
Case 3 $S_d = 2$;
    Set $\left(x'_{1new}, x'_{2new}\right) = \left(x'_1, x'_2\right)$ and $(x_1, x_2) = \left(x'_1, x'_2\right)$. Extract the two secret digits from the reference matrix $M$ corresponding to $\left(x'_{1new}, x'_{2new}\right)$ and $\left(x'_1, x'_2\right)$.
Case 4 $S_d = 5$;
    Set $\left(x'_{1new}, x'_{2new}\right) = \left(x'_1, x'_2\right)$.
    If $\left|x'_1 - x''_1\right| = 2$, then
        $(x_1, x_2) = \left(\left(x'_1 + x''_1\right)/2, x'_2\right)$,
    Else
        Set $(x_1, x_2) = \left(x'_1, \left(x''_1 + x'_2\right)/2\right)$.
        Extract the two secret digits from the reference matrix $M$ corresponding to $\left(x'_{1new}, x'_{2new}\right)$ and $\left(x'_1, x'_2\right)$.
    End
Case 5 $S_d = 4$;
    Set $\left(x'_{1new}, x'_{2new}\right) = \left(x'_1 - \left(x'_1 - x''_1\right)/2, x'_2 - \left(x'_2 - x''_2\right)/2\right)$. Set $(x_1, x_2)$ equal the center pixel that forms a clockwise rotation with the line segment from $\left(x'_1, x'_2\right)$ to $\left(x''_1, x''_2\right)$. Extract the two secret digits from the reference matrix $M$ corresponding to $\left(x'_{1new}, x'_{2new}\right)$ and $\left(x'_1, x'_2\right)$.
Case 6 $S_d = 8$;
    Set $(x_1, x_2) = \left(\left(x'_1 + x''_1\right)/2, \left(x'_2 + x''_2\right)/2\right)$ Set the pixels $\left(x'_{1new}, x'_{2new}\right)$ equal to the pixel that is adjacent to pixels $(x_1, x_2)$ and $(\left(x''_1, x''_2\right)$. The line segment connecting the points $(x'_{1new}, x'_{2new})$ and $(x''_1, x''_2)$ forms a counterclockwise rotation around $(x_1, x_2)$. Extract the two secret digits from the reference matrix $M$ corresponding to $\left(x'_{1new}, x'_{2new}\right)$ and $\left(x'_1, x'_2\right)$.
```

3 The Proposed Scheme

The proposed algorithm is a reversible EMD-based algorithm that uses the general extraction function: $f_e(x, y) = (x + cy)$ mod$m$. In this paper, we set $c = 3$ and $m = 4$. Choosing $m = 4$ means we need to convert the message into the $4-ary$ number system, which requires almost zero computational cost because we can convert two or eight bits of the binary message stream instead of converting the whole message. Thus, the proposed scheme uses the extraction function $f_e(x, y) = (x + 3y)\,mod4$. The neighborhood-set $\psi(0, 0)$ in Fig. 3 shows how the extraction function generates the complete $4 - ary$ number system set. The shaded row in Fig. 3 results from decrementing x by one and incrementing it by 0, 1, or 2 while keeping y intact. The shaded column in Fig. 3 results from decrementing y by one and incrementing it by 0, 1, or 2 while preserving the value of x. To understand the proposed algorithm, consider a cover image I_C consisting of two neighboring pixels (x_1, x_2); we generate two cover images $I_{C1} = I_{C2} = I_C$, as shown in Fig. 4. A secret message digit S_1 is embedded by substituting

x_1 and y_1 in the extraction function and modifying x_1. The embedding process finds the distance $d_1 = (S_1 - f_e(x_1, y_1))\ mod4$, locates this value in the shaded row of the neighborhood set $\psi(0, 0)$ and adjusts x_1 in the first cover image accordingly to obtain the first stego image I'_{C1}. Another secret message digit S_2 is embedded using x_2 and y_2. To do this: find the value $f_e(x_2, y_2) = (x_2 + 3y_2)\ mod4$ and the distance $d_2 = (S_2 - f_e(x_2, y_2))\ mod4$, locate this value in the shaded column of the neighborhood set $\psi(0, 0)$, and modify y_2 in the second cover image accordingly to obtain the second stego image I'_{C2}. Note that the shaded pixels remain intact and can be combined to recover the original cover image achieving reversibility.

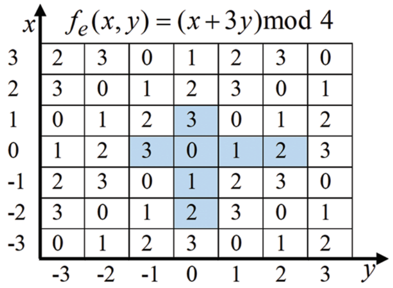
x
$f_e(x,y) = (x+3y)\text{mod } 4$
y

3	2	3	0	1	2	3	0
2	3	0	1	2	3	0	1
1	0	1	2	3	0	1	2
0	1	2	3	0	1	2	3
-1	2	3	0	1	2	3	0
-2	3	0	1	2	3	0	1
-3	0	1	2	3	0	1	2
	-3	-2	-1	0	1	2	3

Figure 3: Neighborhood set

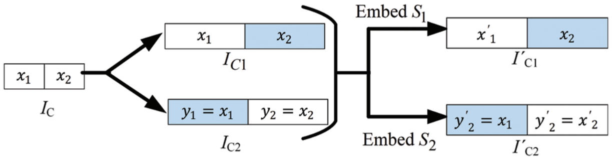

Figure 4: Flow of proposed dual images embedding

In the proposed algorithm, we facilitate the embedding process by defining two novel modification tables to eliminate the search step in the neighborhood set and modify the cover images systematically in a numerically efficient manner. In Fig. 4, the changes to pixels (x_1, x_2) needed to embed the differences d_1 and d_2 are given in the first modification matrix mm_1 given by Eqs. (1) and (2) below.

$$mm_1 = \begin{bmatrix} 0 & 1 & 2 & -1 \\ 0 & 0 & 0 & 0 \end{bmatrix} \tag{1}$$

$$mm_2 = \begin{bmatrix} 0 & 0 & 0 & 0 \\ 0 & -1 & -2 & 1 \end{bmatrix} \tag{2}$$

Eq. (3) finds the stego pixels (x'_1, y'_1):

$$\begin{bmatrix} x'_1 \\ y'_1 \end{bmatrix} = \begin{bmatrix} x_1 \\ y_1 \end{bmatrix} + mm_1(:, d_1) \tag{3}$$

We calculate the stego pixels (x'_2, y'_2) using Eq. (4).

$$\begin{bmatrix} x'_2 \\ y'_2 \end{bmatrix} = \begin{bmatrix} x_2 \\ y_2 \end{bmatrix} + mm_2(:, d_2) \tag{4}$$

For extraction, we find the two secret digits $S_1 = \left(x_1' + 3y_1'\right) mod4$ and $S_2 = \left(x_2' + 3y_2'\right) mod4$. One should notice that the embedding step may change the original embeddable pixel value by a maximum absolute value $\delta = 2$. The change in pixel value may result in overflow or underflow. As outlined in the following subsection, we adjust the border embeddable pixels' values to prevent this problem.

3.1 The Proposed Data Embedding Algorithm

Given the $N \times M$ gray level original cover image I_C and a binary secret message W with length l_W; the embedding procedure consists of the following steps:

Step 1: Obtain the dual cover images I_{C1} and I_{C2} as: $I_{C1} = I_{C2} = I_C$.

Step 2: Classify the dual cover images' pixels into two classes: embeddable pixels and non-embeddable pixels. Embeddable pixels in the first cover image I_{C1} are the pixels $p(i,j)$; $i\ mod(2) = 1,\ i = 1, 2, 3 \ldots M$ and $j = 1, 2, 3 \ldots N$. Embeddable pixels in the second cover image I_{C2} consist of pixels $p(i,j)$; $j\ mod(2) = 0, i = 1, 2, 3 \ldots M$ and$j = 1, 2, 3 \ldots N$. The White pixels (even columns in I_{C1} and odd columns in I_{C2}) in Fig. 5 show the embeddable pixels for the dual cover images, while the shaded pixels (even columns in I_{C1} and odd columns in I_{C2}) are the non-embeddable pixels. The union of the non-embeddable pixels in the two stego images gives the original cover image I_C.

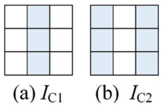

(a) I_{C1} (b) I_{C2}

Figure 5: Embeddable pixels selection

Step 3: Prevent overflow and underflow problems by modifying each embeddable pixel $p(i,j)$ in the cover images I_{C1} and I_{C2} using Eq. (5).

$$p(i,j) = \begin{cases} 255 - \delta, & if\ p(i,j) > 255 - \delta \\ \delta, & if\ p(i,j) < \delta \end{cases} \tag{5}$$

where δ denotes the absolute maximum change to any embeddable pixel. In our algorithm, $\delta = 2$.

Step 4: Sequentially scan the cover images from left to right and top to bottom and embed one $4 - ary$ secret digit using steps 5–8.

Step 5: Get two bits from the binary secret message and find its $4 - ary$ value S_d.

Step 6: Let the current decimal values of the pixels in the preprocessed cover images be: $I_{C1}(i,j) = x$ and $I_{C2}(i,j) = y$. Use Eq. (6) to find the value of the extraction function as:

$$f_e(x, y) = (x + 3y)\, mod4 \tag{6}$$

Step 7: Use Eq. (7) to find the distance d as:

$$d = (S_d - f_e(x, y))\, mod4 \tag{7}$$

Step 8: Find mm_1 and mm_2 as defined by Eqs. (1) and (2), and use Eq. (8) to find the new values of the stego pixels $I'_{C1}(i,j)$ and $I'_{C2}(i,j)$.

$$\begin{bmatrix} I'_{C1}(i,j) \\ I'_{C2}(i,j) \end{bmatrix} = \begin{cases} \begin{bmatrix} x \\ y \end{bmatrix} + mm_1(:,\ d)\,;\ \text{if } I'_{C1}(i,j)\ \ \textit{is embeddable} \\ \begin{bmatrix} x \\ y \end{bmatrix} + mm_2(:,\ d)\,;\ \text{if } I'_{C2}(i,j)\ \ \textit{is embeddable} \end{cases} \tag{8}$$

The result of this process is the two stego images I'_{C1} and I'_{C2}. We repeat steps 4–8 until all secret message bits are embedded.

3.2 The Proposed Data Extraction and Image Recovery Algorithm

Given the dual stego images I'_{C1} and I'_{C2} we recover the original cover image and extract the secret message using the following steps:

Step 1: Classify the stego images' pixels into two classes: embeddable and non-embeddable pixels, in the same manner as in the embedding step. Fig. 6 shows this classification where the white pixels are the embeddable pixels while the shaded pixels are the non-embeddable pixels.

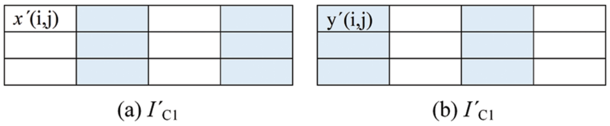

(a) I'_{C1} (b) I'_{C1}

Figure 6: Embeddable pixels classification

Step 2: Recover the original cover image I_C by combining the non-embeddable pixels in the two stego images I'_{C1} and I'_{C2}.

Step 3: Refer to Fig. 6 and let the current decimal values of the stego images' pixels in I'_{C1} and I'_{C2} be $p'_{C1}(i,j) = x'$ and $p'_{C2}(i,j) = y'$. Extract the secret message digit using Eq. (9).

$$S_d = (x' + 3y')\,mod4 \tag{9}$$

Step 4: Find the binary value of S_d and concatenate it to the extracted binary message.
Extract all secret message digits by repeating steps 3 and 4.

3.3 Numerical Example

We conclude this section by giving a numerical example to illustrate the operational steps of the proposed reversible DHT. Fig. 7 shows a 1 × 2 original cover image I_C and the corresponding dual cover images I_{C1} and I_{C2}. The shaded pixels in Fig. 7 are non-embeddable, while the white pixels are embeddable. The preprocessing step replaces the value 255 in the cover image I_{C1} by 253. Fig. 8 shows the resulting preprocessed cover images.

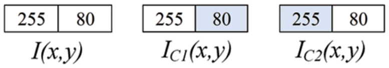

Figure 7: Original and dual cover images

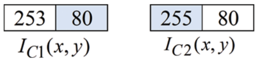

253	80		255	80
$I_{C1}(x,y)$			$I_{C2}(x,y)$	

Figure 8: Preprocessed dual cover images

Given the binary secret message $W = [1011]$, convert every two binary bits into its $4-ary$ format. The resulting secret message is $S = [23]$. The digits of the secret message S are embedded in the dual cover images as follows:

Assign the value of the first pixel in I_{C1} as: $x = p_{C1}(1,1) = 253$ and assign the value of the first pixel in I_{C2} as: $y = p_{C2}(1,1) = 255$ → Use Eq. (6) to find the value of the extraction function, $f_e = (x+3y)\,mod4 = 2$ → Get the first secret digit $S_1 = 2$→ Use Eq. (7) to find the distance $d = (S_1 - f_e)\,mod4 = 0$. → use Eq. (8) to find the stego images pixels as:

$$\begin{bmatrix} p'_{C1}(1,1) \\ p'_{C2}(1,1) \end{bmatrix} = \begin{bmatrix} x \\ y \end{bmatrix} + mm_1(:,d) = \begin{bmatrix} 253 \\ 255 \end{bmatrix} + \begin{bmatrix} 0 \\ 0 \end{bmatrix} = \begin{bmatrix} 253 \\ 255 \end{bmatrix}.$$

Assign the value of the next pixel in I_{C1} as: $x = p_{C1}(1,2) = 80$ → assign the value of the first pixel in I_{C2} as: $y = p_{C2}(1,2) = 80$.→ use Eq. (6) to find the value of the extraction function $f_e = (x+3y)\,mod4 = 0$→ Get the next secret digit $S_2 = 3$→ Use Eq. (7) to find the distance $d = (S_2 - f_e)\,mod4 = 3$. → use Eq. (8) to find the stego images pixels as:

$$\begin{bmatrix} p'_{C1}(1,2) \\ p'_{C2}(1,2) \end{bmatrix} = \begin{bmatrix} x \\ y \end{bmatrix} + mm_2(:,d) = \begin{bmatrix} 80 \\ 80 \end{bmatrix} + \begin{bmatrix} 0 \\ 1 \end{bmatrix} = \begin{bmatrix} 80 \\ 80 \end{bmatrix} + \begin{bmatrix} 0 \\ 1 \end{bmatrix} = \begin{bmatrix} 80 \\ 81 \end{bmatrix}.$$

Fig. 9 shows the resulting dual stego images.

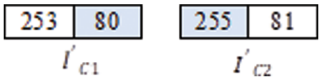

253	80		255	81
I'_{C1}			I'_{C2}	

Figure 9: Dual stego images

For extraction, starting with dual stego images in Fig. 9, the original cover image is obtained by combining the shaded columns in I'_{C1}, and I'_{C2}. We extract the hidden message as follows: Assign the value of the first pixel in I'_{C1} as: $x = p'_{C1}(1,1) = 253$ and assign the value of the first pixel in I'_{C2} as: $y = p_{C2}(1,1) = 255$. → Use Eq. (9) to find the value of the first hidden digit as $S_1 = (x+3y)\,mod4 = 2$ → Convert S_1 to its two bits binary equivalent $S_{1d} = 10$→ Concatenate this to the extracted binary message. Assign the value of the next pixel in I'_{C1} as: $x = p'_{C1}(1,2) = 80$ and assign the value of the next pixel in I'_{C2} as: $y = p'_{C2}(1,2) = 81$. → use Eq. (9) to find the value of the next hidden digit as $S_2 = (x+3y)\,mod4 = 3$ → Convert S_2 to its two-bit binary equivalent $S_{2d} = 11$→ Concatenate this to the extracted binary message. The resulting extracted message: $S_{ext} = [S_{1d}S_{2d}] = [1011]$ is equivalent to the embedded message W.

4 Experimental Results

This section presents the simulation results of the proposed technique. To measure the quality of the stego images, we use the PSNR values of the stego images. The PSNR between an $M \times N$ original cover image I and the stego image I', is given by Eq. (10) [45]:

$$PSNR(I,I') = 10\ \log_{10} \frac{M \times N \times (255)^2}{\sum_{i=1}^{M}\sum_{j=1}^{N}(X(i,j) - I_s(i,j))^2}\ \text{dB} \tag{10}$$

We use the embedding rate as a measure of the data hiding capacity. The embedding rate R is given by Eq. (11).

$$R = EB/\left(2 \times M \times N\right) \tag{11}$$

where EB represents the total number of the embedded binary bits.

We used the CPU time as a measure to evaluate the numerical efficiency. In our simulations, we used twelve 512 × 512 grayscale cover images. The secret message is a randomly generated binary secret message using MatLab. Fig. 10 shows the twelve test images. We performed our simulations on a personal computer with an Intel(R) Core(T.M.) i7-6700 CPU @ 3.40 GHz and 8 G.B. memory.

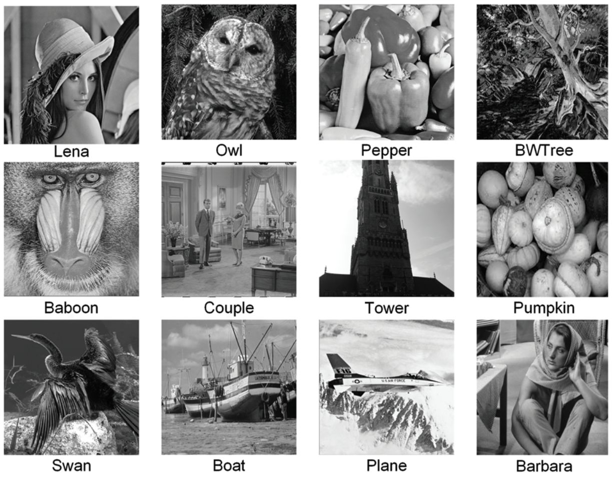

Figure 10: Test images

4.1 Performance Evaluation of the Proposed Technique

Fig. 11 shows the stego images at the maximum embedding rate. The high quality of the stego images is clear, and the human eye can detect no traces of any artifacts.

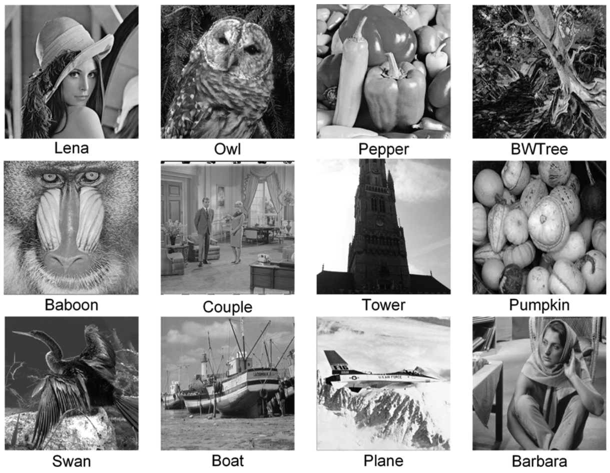

Figure 11: Stego images

Table 1 gives the main features of our technique. The high quality of the stego images is evident via an average PSNR value of more than 49 dB. In addition, Table 1 also shows that the average absolute distortion in the pixels is about 0.5/pixel. Moreover, Table 1 also shows that, at the maximum embedding rate, our algorithm achieved a high average PSNR value of 49 dB. We conducted another experiment to investigate the PSNR values of the stego images against different embedding rates. Fig. 12 shows the results for the Lena image, where the PSNR values for both stego images ranged from 80 dB when the embedding rate is 1/16 bpp to 49 dB when the embedding rate is one bpp. An essential feature of our algorithm is that the PSNR values are practically identical for both stego images. This feature improves security. In addition, the PSNR values are almost identical for all test images. This shows that the performance of our technique does not depend on the cover image. Our technique embeds one $4 - ary$ digit (two binary bits) in each pixel pair in the cover images resulting in an embedding rate of one bpp, as Table 1 shows. Table 2 demonstrates the numerical efficiency of our technique. The numerical efficiency of our technique resulting from using the modification tables and eliminating the search step is evident in the short embedding and extraction times shown in Table 2.

Table 1: Performance and comparison with related work

Image	PSNR (dB)				Average absolute error				Embedding rate (BPP)	
	Ours		[31]		Ours		[31]		Ours	[31]
	S1	S2	S1	S2	S1	S2	S1	S2		
Lena	49.37	49.37	50.65	49.09	0.502	0.499	0.561	0.561	1	1
Owl	49.37	49.37	50.64	49.10	0.502	0.499	0.561	0.561	1	1
Peppers	49.37	49.37	50.66	49.10	0.502	0.499	0.562	0.562	1	1
BW-Tree	49.28	49.35	50.68	49.13	0.506	0.500	0.555	0.555	1	0.993
Baboon	49.37	49.37	50.66	49.10	0.502	0.499	0.560	0.560	1	1
Couple	49.29	49.28	50.71	49.16	0.506	0.503	0.555	0.555	1	0.988
Tower	48.67	47.48	51.27	49.73	0.535	0.600	0.486	0.486	1	0.865
Pumpkin	49.29	49.35	50.67	49.13	0.506	0.499	0.556	0.556	1	0.994
Swan	49.26	49.04	50.75	49.21	0.507	0.514	0.554	0.554	1	0.977
Boat	49.37	49.37	50.65	49.09	0.502	0.499	0.560	0.559	1	1
Plane	49.37	49.37	50.63	49.10	0.502	0.499	0.560	0.559	1	1
Barbara	49.37	49.37	50.66	49.10	0.502	0.499	0.560	0.560	1	1
Average	**29.49**	**49.19**	**50.71**	**49.17**	**0.502**	**0.508**	**0.553**	**0.553**	**1**	**0.986**

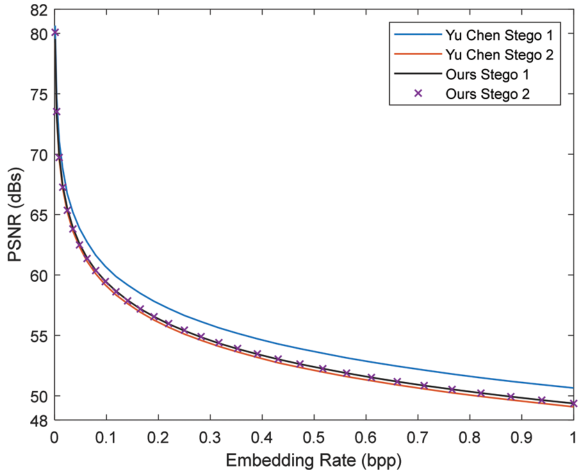

Figure 12: PSNR *vs.* embedding rate performance lena image

Table 2: CPU time (s) comparison with related work

Image	Embedding CPU time		Extraction CPU time	
	Ours	[31]	Ours	[31]
Lena	0.03125	0.3125	0.03125	0.03125
Owl	0.015625	0.140625	0.015625	0.015625
Peppers	0.03125	0.15625	0.015625	0.015625
BW-Tree	0.03125	0.15625	0.015625	0.015625
Baboon	0.03125	0.140625	0.03125	0.015625
Couple	0.03125	0.140625	0.015625	0.03125
Tower	0.03125	0.125	0.015625	0.03125
Pumpkin	0.03125	0.15625	0.015625	0.03125
Swan	0.03125	0.140625	0.03125	0.03125
Boat	0.03125	0.171875	0.015625	0.015625
Plane	0.03125	0.140625	0.015625	0.015625
Barbara	0.03125	0.140625	0.03125	0.03125
Average	**0.030048**	**0.1586538**	**0.020432**	**0.024038**

4.2 Performance Comparisons with Related Work

Table 1 also compares our technique with [31] in terms of PSNR values, average absolute error, and embedding rates. The average embedding rate of our technique is one bpp, while that of [31] is 0.9859 bpp. In obtaining these results, we converted each byte of the binary message to its $5 - ary$ value in [31] and $4 - ary$ value in our technique. The PSNR values for both techniques are close. However, The PSNR values of our two stego images are almost identical, while that of [31] are slightly different. Fig. 12 gives the PSNR values *vs.* Embedding rate for both techniques and shows that the PSNR values of our two stego images lie between the two stego images' PSNR values in [31]. Another feature of our technique is numerical efficiency and simplicity. Instead of using a 256 × 256 neighborhood matrix in the embedding and extraction phases in [31], we only need two 2 × 4 lookup tables, resulting in significant savings in storage and numerical calculations. Although the execution time depends on the status of the operating system and may vary from one run to another, Table 2 shows that the embedding CPU time of our technique is one-fifth of that of [31]. Table 2 also shows that the extraction CPU time of our technique is 0.8 that of [31]. Table 3 compares the PSNR values of our technique with that of [24,31,42,43]. These techniques have maximum embedding rates of 1, 1, 1.25, and 1 bpp, respectively. For a fair comparison, Table 3 gives PSNR values at the same embedding rate of 1 bpp. Our technique and [24] give equal PSNR values for both stego images making them less susceptible to detection by intruders. The PSNR value of the two stego images in [31,42,43] by 1, 5, and 5 dB, respectively, making it more vulnerable to detection. Overall, our technique outperforms other techniques in terms of image quality, simplicity, and numerical efficiency.

Table 3: PSNR value (dB) comparisons for the two stego images (dB)

Image	[24]		[31]		[42]		[43]		Ours	
	S1	S2	S1	S2	S1	S2	S1	S2	S1	S2
Airplane	45.32	45.34	50.63	49.10	50..41	45.47	51.68	45.73	49.41	49.37
Baboon	45.34	45.34	50.66	49.10	50.42	45.46	51.72	45.71	49.37	49.37
Barbara	45.35	45.34	50.66	49.10	50.45	45.45	51.73	45.70	49.37	49.37
Lena	45.32	45.32	50.65	49.09	50.39	45.47	51.69	45.70	49.37	49.37
Peppers	45.33	45.34	50.66	49.10	50.45	45.45	51.73	45.70	49.37	49.37
Average	**45.32**	**45.32**	**50.65**	**49.10**	**50.43**	**45.46**	**51.71**	**45.71**	**49.37**	**49.37**

5 Conclusion

This paper presented a new reversible RDHT based on EMD. The proposed technique is simple and numerically efficient. It limits image distortions and increases stego image quality and transparency. Each pixel pair of the two stego images (one pixel from each stego image) hides one $4 - ary$ secret digit by modifying only one pixel with a maximum distortion of two resulting in an embedding rate of one bpp. Using the two novel 2 × 4 lookup tables highly reduces numerical calculations by eliminating the numerically demanding search step in similar techniques. The embedding strategy enabled direct reversibility at almost zero computational cost. Increased security is achieved by transmitting the two stego images on separate channels so that only the receiver with both stego images and the embedding sequence can extract the secret message. Experimental results demonstrate the high quality of the two stego images with more than 49 dB average PSNR values. Experimental results also show that the embedding CPU time of our technique is one-fifth of that of [31]. The extraction CPU time of our technique is 0.8 that of [31].

Funding Statement: The author received no funding for this study.

Conflicts of Interest: The author declares that he has no conflicts of interest to report regarding the present study.

References

[1] Z. Yin, Y. Peng and Y. Xiang, "Reversible data hiding in encrypted images based on pixel prediction and bit-plane compression," *IEEE Transactions on Dependable and Secure Computing*, vol. 19, no. 2, pp. 992–1002, 2022.

[2] I. J. Cox, M. L. Miller, J. A. Bloom, J. Fridrich and T. Kalker, "Chapter 1-Introduction," in *The Morgan Kaufmann Series in Multimedia Information and Systems*, 2nd edition, Morgan Kaufmann, Amsterdam, Netherlands: Elsevier Publishing company, pp. 1–13, 2008.

[3] A. A. Mohammad, A. Al-Haj and M. Farfoura, "An improved capacity data hiding technique based on image interpolation," *Multimedia Tools and Applications*, vol. 78, no. 6, pp. 7181–7205, 2018.

[4] Z. S. Younus and M. K. Hussain, "Image steganography using exploiting modification direction for compressed encrypted data," *Journal of King Saud University-Computer and Information Sciences*, vol. 34, no. 6, pp. 2951–2963, 2022.

[5] C. -M. Wang, N. -I. Wu, C. -S. Tsai and M. -S. Hwang, "A high quality steganographic method with pixel-value differencing and modulus function," *Journal of Systems and Software*, vol. 81, no. 1, pp. 150–158, 2008.

[6] K. -H. Jung and K. -Y. Yoo, "Improved exploiting modification direction method by modulus operation," *International Journal of Signal Processing Image Processing and Pattern Recognition*, vol. 2, no. 3, pp. 79–87, 2009.

[7] W. Kou, "Image hiding by square fully exploiting modification directions," *Journal of Information Hiding and Multimedia Signal Processing*, vol. 4, no. 1, pp. 128–137, 2013.

[8] X. Zhang and S. Wang, "Efficient steganographic embedding by exploiting modification direction," *IEEE Communications Letters*, vol. 10, no. 11, pp. 781–783, 2006.

[9] C. -F. Lee, Y. -R. Wang and C. -C. Chang, "A steganographic method with high embedding capacity by improving exploiting modification direction," in *Third Int. Conf. on Intelligent Information Hiding and Multimedia Signal Processing (IIH-MSP 2007)*, Kaohsiung, Taiwan, pp. 497–500, 2007.

[10] R. -M. Chao, H. -C. Wu, C. -C. Lee and Y. -P. Chu, "A novel image data hiding scheme with diamond encoding," *EURASIP Journal on Information Security*, vol. 2009, pp. 1–9, 2009.

[11] R. Rasiyath, "Data embedding and extracting using pixel pair matching with potential masking," *Indian Journal of Applied Research*, vol. 3, no. 7, pp. 272–276, 2011.

[12] T. D. Kieu and C. -C. Chang, "A steganographic scheme by fully exploiting modification directions," *Expert Systems with Applications*, vol. 38, no. 8, pp. 10648–10657, 2011.

[13] W. -C. Kuo and M. -C. Kao, "A steganographic scheme based on formula fully exploiting modification directions," *IEICE Transactions on Fundamentals of Electronics, Communications and Computer Sciences*, vol. E96.A, no. 11, pp. 2235–2243, 2013.

[14] S. -Y. Shen and L. -H. Huang, "A data hiding scheme using pixel value differencing and improving exploiting modification directions," *Computers & Security*, vol. 48, pp. 131–141, 2015.

[15] T. D. Sairam and K. Boopathybagan, "An improved high capacity data hiding scheme using pixel value adjustment and modulus operation," *Multimedia Tools and Applications*, vol. 79, no. 23–24, pp. 17003–17013, 2019.

[16] S. Atawneh, A. Almomani, H. Al Bazar, P. Sumari and B. Gupta, "Secure and imperceptible digital image steganographic algorithm based on diamond encoding in DWT domain," *Multimedia Tools and Applications*, vol. 76, no. 18, pp. 18451–18472, 2016.

[17] Z. Li and Y. He, "Steganography with pixel-value differencing and modulus function based on PSO," *Journal of Information Security and Applications*, vol. 43, pp. 47–52, 2018.

[18] S. Saha, A. Chakraborty, A. Chatterjee, S. Dhargupta, S. K. Ghosal *et al.,* "Extended exploiting modification direction based steganography using hashed-weightage array," *Multimedia Tools and Applications*, vol. 79, no. 29–30, pp. 20973–20993, 2020.

[19] J. -H. Horng, S. Xu, C. -C. Chang and C. -C. Chang, "An efficient data-hiding scheme based on multidimensional mini-sudoku," *Sensors*, vol. 20, no. 9, pp. 2739, 2020.

[20] H. -H. Liu, P. -C. Su and M. -H. Hsu, “An improved steganography method based on least-significant-bit substitution and pixel-value differencing,” *KSII Transactions on Internet and Information Systems*, vol. 14, no. 11, pp. 4537–4556, 2020.

[21] C. -F. Lee, J. -J. Shen, S. Agrawal, Y. -X. Wang and Y. -H. Lee, “Data hiding method based on 3D magic cube,” *IEEE Access*, vol. 8, pp. 39445–39453, 2020.

[22] R. Atta, M. Ghanbari and I. Elnahry, “Advanced image steganography based on exploiting modification direction and neutrosophic set,” *Multimedia Tools and Applications*, vol. 80, no. 14, pp. 21751–21769, 2021.

[23] J. J. Ranjani and F. Zaid, “Pseudo magic cubes: A multidimensional data hiding scheme exploiting modification directions for large payloads,” *Computers & Electrical Engineering*, vol. 89, pp. 106928, 2021.

[24] C. -C. Chang, T. Kieu and Y. -C. Chou, “Reversible data hiding scheme using two steganographic images,” in *Proc. of TENCON 2007-2007 IEEE Region 10 Conf.*, Taipei, Taiwan, pp. 1–4, 2007.

[25] C. -C. Chang, T. -C. Lu, G. Horng, Y. -H. Huang and Y. -M. Hsu, “A high payload data embedding scheme using dual stego-images with reversibility,” in *Proc. of 2013 9th Int. Conf. on Information, Communications & Signal Processing*, Tainan, Taiwan, pp. 1–5, 2013.

[26] C. Qin, C. -C. Chang and T. -J. Hsu, “Reversible data hiding scheme based on exploiting modification direction with two steganographic images,” *Multimedia Tools and Applications*, vol. 74, no. 15, pp. 5861–5872, 2014.

[27] J. -Y. Hsiao, A. -C. Pan and P. -Y. Chen, “An adaptive reversible data hiding scheme using dual stego-image,” *International Journal of Computers and Applications*, vol. 43, no. 3, pp. 282–291, 2018.

[28] C. -F. Lee, C. -Y. Weng and K. -C. Chen, “An efficient reversible data hiding with reduplicated exploiting modification direction using image interpolation and edge detection,” *Multimedia Tools and Applications*, vol. 76, no. 7, pp. 9993–10016, 2016.

[29] J. -Y. Lin, Y. Chen, C. -C. Chang and Y. -C. Hu, “Dual-image-based reversible data hiding scheme with integrity verification using exploiting modification direction,” *Multimedia Tools and Applications*, vol. 78, no. 18, pp. 25855–25872, 2019.

[30] X. Chen and W. Guo, “Reversible data hiding scheme based on fully exploiting the orientation combinations of dual stego-images,” *International Journal of Network Security*, vol. 22, no. 1, pp. 126–135, 2020.

[31] Y. Chen, J. Lin, C. C. Chang and Y. C. Hu, “Reversibly hiding data using dual images scheme based on EMD data hiding method,” *International Journal of Computational Science and Engineering*, vol. 21, no. 4, pp. 583, 2020.

[32] J. -Y. Lin, J. -H. Horng, C. -C. Chang and Y. -H. Li, “Asymmetric orientation combination for reversible and authenticable data hiding of dual stego-images,” *Symmetry*, vol. 14, no. 4, pp. 819, 2022.

[33] S. Subburam, S. Selvakumar and S. Geetha, “High performance reversible data hiding scheme through multilevel histogram modification in lifting integer wavelet transform,” *Multimedia Tools and Applications*, vol. 77, no. 6, pp. 7071–7095, 2017.

[34] S. Kim, X. Qu, V. Sachnev and H. J. Kim, “Skewed histogram shifting for reversible data hiding using a pair of extreme predictions,” *IEEE Transactions on Circuits and Systems for Video Technology*, vol. 29, no. 11, pp. 3236–3246, 2019.

[35] L. -C. Huang, S. -F. Chiou and M. -S. Hwang, “A reversible data hiding based on histogram shifting of prediction errors for two-tier medical images,” *Informatica*, vol. 32, no. 1, pp. 69–84, 2021.

[36] J. -Y. Lin, Y. Liu and C. -C. Chang, “A real-time dual-image-based reversible data hiding scheme using turtle shells,” *Journal of Real-Time Image Processing*, vol. 16, no. 3, pp. 673–684, 2019.

[37] H. Yu, R. Wang, L. Dong, D. Yan, Y. Gong *et al.,* “A high-capacity reversible data hiding scheme using dual-channel audio,” *IEEE Access*, vol. 8, pp. 162271–162278, 2020.

[38] X. Chen and C. Hong, “An efficient dual-image reversible data hiding scheme based on exploiting modification direction,” *Journal of Information Security and Applications*, vol. 58, pp. 102702, 2021.

[39] X. -Z. Xie and C. -C. Chang, “Hiding data in dual images based on turtle shell matrix with high embedding capacity and reversibility,” *Multimedia Tools and Applications*, vol. 80, no. 30, pp. 36567–36584, 2021.

[40] S. Chen and C. -C. Chang, “Reversible data hiding based on three shadow images using rhombus magic matrix,” *Journal of Visual Communication and Image Representation*, vol. 76, pp. 103064, 2021.

[41] J. -Y. Lin, J. -H. Horng and C. -C. Chang, “A reversible and authenticable secret sharing scheme using dual images,” *Multimedia Tools and Applications*, vol. 81, no. 13, pp. 17527–17545, 2022.

[42] C. -C. Chang, G. -D. Su, C. -C. Lin and Y. -H. Li, “Position-aware guided hiding data scheme with reversibility and adaptivity for dual images,” *Symmetry*, vol. 14, no. 3, pp. 509, 2022.

[43] Y. Liu and C. C. Chang, “A turtle shell-based visual secret sharing scheme with reversibility and authentication,” *Multimedia Tools and Applications*, vol. 19, no. 3, pp. 25295–25310, 2018.

[44] A. Shamir and M. -S. Hwang, “How to share a secret,” *Communications of the ACM*, vol. 22, no. 11, pp. 612–613, 1979.

[45] D. R. Setiadi, “PSNR *vs.* SSIM: Imperceptibility quality assessment for image steganography,” *Multimedia Tools and Applications*, vol. 80, no. 6, pp. 8423–8444, 2020.